

Maximum Reduced Proper Motion Method: Detection of New Nearby Ultracool Dwarfs

N. Phan-Bao^{1,*}

Department of Physics, HCMIU, Vietnam National University Administrative Building, Block 6, Linh Trung Ward, Thu Duc District, HCM, Vietnam

Received ..., accepted ...

Published online ...

Key words stars: low mass, brown dwarfs – solar neighborhood – stars: distances – stars: fundamental parameters

In this paper, we describe how to use the Maximum Reduced Proper Motion method (Phan-Bao et al. 2003) to detect 57 nearby L and late-M dwarfs ($d_{\text{phot}} \leq 30$ pc): 36 of them are newly discovered. Spectroscopic observations of 43 of the 57 ultracool dwarfs were previously reported in Martín et al. (2010). These ultracool dwarfs were identified by color criteria in $\sim 5,000$ square degrees of the DENIS database and then further selected by the method for spectroscopic follow-up to determine their spectral types and spectroscopic distances. We also report here our newly measured proper motions of these ultracool dwarfs from multi-epoch images found in public archives (ALADIN, DSS, 2MASS, DENIS), with at least three distinct epochs and time baselines of 2 to 46 years.

© WILEY-VCH Verlag GmbH & Co. KGaA, Weinheim

1 INTRODUCTION

Nearby stars are the brightest representatives of their class, and therefore provide observational benchmarks for stellar physics. This is particularly true for intrinsically faint objects, such as stars at the bottom of the main sequence, and brown dwarfs (BDs).

In the last decade, many nearby ($d \leq$

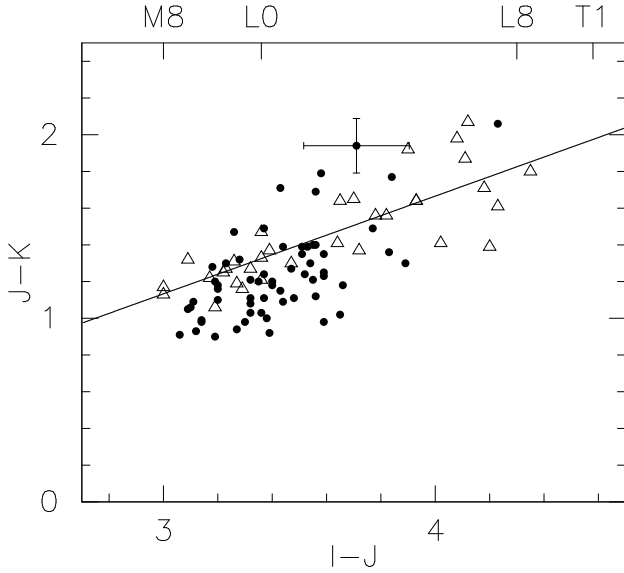


Fig. 1 $(I - J, J - K)$ color-color diagram for our 60 late-M and L dwarf candidates (Table 1), plotted as solid circles, as well as known late-M and L dwarfs (see Table 1 in Phan-Bao et al. 2008; plotted as open triangles). The line represents our linear fit to the colors of the literature dwarfs: $J - K = -0.462 + 0.532(I - J)$, $\sigma = 0.15$.

jects which matched $|b_{II}| \geq 15^\circ$ (high Galactic latitude) and $I - J \geq 3.0$ (expected spectral type later than M8, see Leggett 1992). We then required that the position of the candidates in the $(I - J, J - K)$ color-color diagram be within $J - K = \pm 0.5$ mag of our linear fit to the locus of ultracool dwarfs (Fig. 1).

At this point we filtered out all candidates within the boundaries of the Magellanic Clouds (Cioni et al. 2000) and of known high-latitude molecular clouds (see Table 2 of Cruz et al. 2003 and references therein). This eliminated most red giants and reddened blue stars, at the obvious cost of losing the cool dwarfs which happen to overlap a cloud. We then computed photometric distances from the following $(I - J, M_J)$ relation as given in Phan-Bao et al. (2008) and retained the candidates with $d_{\text{phot}} \leq 30$ pc:

$$M_J = a_0 + a_1(I - J) + a_2(I - J)^2 + a_3(I - J)^3 + a_4(I - J)^4 \quad (1)$$

where $a_0 = 130.164$, $a_1 = -124.899$, $a_2 = 46.948$, $a_3 = -7.4842$, $a_4 = 0.4341$, valid for $3.0 \leq I - J \leq 6.0$. The rms dispersion around that fit is 0.30 mag, corresponding to a 14% error on distances.

Before measuring proper motions, which is needed for the use of the MRPM method to discriminate between nearby dwarfs and distant giants, we cross-identified the bright candidates ($I < 13.0$, $d_{\text{phot}} \ll 30$ pc) with both SIMBAD and the catalogs of red variable stars (e.g. Pojmanski et al. 2005; Samus et al. 2004) in VIZIER. As expected, all bright candidates are previously recognized giants. This left 60 ul-

tracool dwarf candidates (Table 1) for which we needed to measure proper motions.

3 PROPER MOTION MEASUREMENTS

We queried ALADIN¹ and the Digital Sky Survey (DSS) server² for publically available scanned plates containing these candidates. Both ALADIN and the DSS archive provide access to the plates of the POSS-I (R-band), SERC-R (R-band), SERC-I (I-band), POSS-II F (R-band), and POSS-II N (I-band) surveys. ALADIN additionally contains digitized images of the ESO-R survey (R-band), which often extend the time baseline enough to significantly reduce the standard error of our proper motion measurements. Forty candidates were detected in R-band. We used SEXTRACTOR (Bertin & Arnouts 1996) to extract coordinates of our targets from all available digitized images. We then determined proper motions through a least-square fit to the positions at the three to five available epochs with time baselines spanning 2–46 yr, including DENIS and 2MASS³. A few objects with short baselines (e.g., DENIS 0230–0953, Table 2) have large errors. New images for those would greatly extend their epoch coverage and would pinpoint their proper motion. Most of the measurements are of much better quality however, and the lowest confidently measured proper motions are ~ 40 mas yr⁻¹ (DENIS 0407–2348, DENIS 0605–2342).

Table 2 and 3 list these proper motions and the associated standard errors. These tables include 38 objects with $\mu \geq 0.1''\text{yr}^{-1}$ and 22 with $\mu \leq 0.1''\text{yr}^{-1}$. Eight of the 38 objects were previously reported as high-pm ultracool dwarfs in Deacon et al. (2005).

4 L AND LATE-M DWARF CANDIDATES SELECTED BY MAXIMUM REDUCED PROPER MOTION

As in our search for nearby mid-M dwarfs (Phan-Bao et al. 2003), we use the MRPM method to reject giants. This method uses the reduced proper motion ($H = M + 5 \log(V_t / 4.74) = m + 5 + \log(\mu)$) versus color diagram, where nearby ultracool dwarfs and distant giants segregate very cleanly. We use the color-magnitude relation of giants to compute the maximum reduced proper motion that a red giant can have at a given color by setting its tangential velocity to the Galactic escape velocity, for which we adopt a conservative 800 km s⁻¹. We then declare any object with a reduced proper motion well above ($> 3\sigma$) that value for its color to be a dwarf.

To use this method here for the cooler dwarfs (M8–L8), we had to extend the maximum reduced proper motion curve of giants towards redder colors ($I - J \geq 3.0$), adding

¹ <http://aladin.u-strasbg.fr/java/nph-aladin.pl>

² http://archive.stsci.edu/cgi-bin/dss_plate_finder

³ <http://cdsweb.u-strasbg.fr/viz-bin/VizieR>

Table 1 60 DENIS red objects

| DENIS name | α_{2000} | δ_{2000} | Epoch | I | $I - J$ | $J - K$ | err I | err J | err K |
|-----------------|-----------------|-----------------|----------|-------|---------|---------|---------|---------|---------|
| J0000286–124514 | 00 00 28.69 | –12 45 14.7 | 1998.564 | 16.16 | 3.09 | 1.05 | 0.08 | 0.11 | 0.11 |
| J0006579–643654 | 00 06 57.92 | –64 36 54.2 | 1998.860 | 16.71 | 3.28 | 1.32 | 0.12 | 0.09 | 0.11 |
| J0014554–484417 | 00 14 55.44 | –48 44 17.1 | 1996.669 | 17.54 | 3.56 | 1.40 | 0.13 | 0.08 | 0.13 |
| J0028554–192716 | 00 28 55.44 | –19 27 16.6 | 1998.784 | 17.61 | 3.66 | 1.18 | 0.18 | 0.18 | 0.17 |
| J0031192–384035 | 00 31 19.28 | –38 40 35.8 | 1999.748 | 17.62 | 3.52 | 1.24 | 0.14 | 0.10 | 0.15 |
| J0050244–153818 | 00 50 24.41 | –15 38 18.9 | 1999.715 | 16.86 | 3.20 | 1.10 | 0.10 | 0.10 | 0.11 |
| J0053189–363110 | 00 53 18.97 | –36 31 10.5 | 2000.885 | 18.10 | 3.89 | 1.30 | 0.19 | 0.12 | 0.16 |
| J0055005–545026 | 00 55 00.53 | –54 50 26.3 | 2000.896 | 17.12 | 3.38 | 1.00 | 0.11 | 0.20 | 0.15 |
| J0116529–645557 | 01 16 52.90 | –64 55 57.1 | 1996.661 | 17.90 | 3.46 | 1.28 | 0.16 | 0.10 | 0.17 |
| J0128266–554534 | 01 28 26.64 | –55 45 34.4 | 2000.863 | 17.07 | 3.26 | 1.47 | 0.16 | 0.12 | 0.13 |
| J0147327–495448 | 01 47 32.77 | –49 54 48.0 | 2000.885 | 16.05 | 3.14 | 0.97 | 0.07 | 0.09 | 0.07 |
| J0206566–073519 | 02 06 56.68 | –07 35 19.8 | 1999.907 | 17.92 | 3.58 | 1.35 | 0.17 | 0.11 | 0.15 |
| J0213371–134322 | 02 13 37.12 | –13 43 22.3 | 1998.808 | 17.64 | 3.36 | 1.03 | 0.17 | 0.16 | 0.18 |
| J0227102–162446 | 02 27 10.28 | –16 24 46.8 | 1998.805 | 17.04 | 3.37 | 1.49 | 0.11 | 0.12 | 0.18 |
| J0230450–095305 | 02 30 45.01 | –09 53 05.1 | 2000.831 | 18.24 | 3.56 | 1.69 | 0.21 | 0.18 | 0.15 |
| J0240121–530552 | 02 40 12.11 | –53 05 52.5 | 1998.932 | 18.18 | 3.83 | 1.36 | 0.22 | 0.10 | 0.16 |
| J0254058–193452 | 02 54 05.81 | –19 34 52.3 | 2000.904 | 16.30 | 3.19 | 1.20 | 0.08 | 0.08 | 0.10 |
| J0301488–590302 | 03 01 48.84 | –59 03 02.3 | 1996.817 | 16.80 | 3.37 | 1.11 | 0.10 | 0.08 | 0.09 |
| J0304322–243513 | 03 04 32.28 | –24 35 13.7 | 1996.934 | 17.29 | 3.32 | 1.03 | 0.12 | 0.09 | 0.17 |
| J0325293–431229 | 03 25 29.37 | –43 12 29.8 | 2000.743 | 17.48 | 3.32 | 1.21 | 0.15 | 0.10 | 0.16 |
| J0407089–234829 | 04 07 08.91 | –23 48 29.9 | 1998.742 | 16.80 | 3.20 | 1.18 | 0.09 | 0.15 | 0.17 |
| J0419556–402534 | 04 19 55.65 | –40 25 34.3 | 2000.888 | 17.34 | 3.41 | 1.20 | 0.11 | 0.10 | 0.13 |
| J0427270–112713 | 04 27 27.09 | –11 27 13.8 | 1996.948 | 16.67 | 3.14 | 0.99 | 0.13 | 0.08 | 0.12 |
| J0436205–421851 | 04 36 20.53 | –42 18 51.7 | 2000.880 | 18.00 | 3.55 | 1.30 | 0.17 | 0.12 | 0.16 |
| J0501005–770549 | 05 01 00.53 | –77 05 49.0 | 1999.795 | 17.16 | 3.27 | 0.95 | 0.11 | 0.10 | 0.15 |
| J0526434–445544 | 05 26 43.47 | –44 55 44.7 | 1996.954 | 17.62 | 3.59 | 1.25 | 0.14 | 0.10 | 0.14 |
| J0605019–234227 | 06 05 01.93 | –23 42 27.2 | 1999.129 | 17.89 | 3.51 | 1.35 | 0.14 | 0.09 | 0.15 |
| J0624458–452156 | 06 24 45.87 | –45 21 56.1 | 1997.082 | 18.32 | 3.84 | 1.77 | 0.19 | 0.11 | 0.13 |
| J0627401–391933 | 06 27 40.17 | –39 19 33.2 | 2000.893 | 17.50 | 3.41 | 1.18 | 0.13 | 0.11 | 0.15 |
| J0641184–432233 | 06 41 18.41 | –43 22 33.3 | 1998.959 | 16.97 | 3.23 | 1.31 | 0.08 | 0.08 | 0.11 |
| J0703238–611004 | 07 03 23.84 | –61 10 04.7 | 1996.101 | 17.91 | 3.44 | 1.39 | 0.19 | 0.11 | 0.16 |
| J0719317–505141 | 07 19 31.76 | –50 51 41.4 | 1996.117 | 17.44 | 3.44 | 1.09 | 0.11 | 0.09 | 0.14 |
| J0921141–210445 | 09 21 14.10 | –21 04 45.5 | 2001.132 | 16.50 | 3.65 | 1.02 | 0.09 | 0.08 | 0.10 |
| J1019245–270717 | 10 19 24.58 | –27 07 17.5 | 1997.189 | 16.90 | 3.33 | 1.08 | 0.10 | 0.08 | 0.15 |
| J1115297–242934 | 11 15 29.72 | –24 29 34.8 | 1998.222 | 16.50 | 3.12 | 0.93 | 0.08 | 0.07 | 0.15 |
| J1206501–393725 | 12 06 50.12 | –39 37 25.9 | 1996.109 | 17.67 | 3.36 | 1.19 | 0.16 | 0.10 | 0.16 |
| J1234018–112407 | 12 34 01.89 | –11 24 07.2 | 1999.463 | 18.22 | 3.59 | 1.23 | 0.19 | 0.13 | 0.20 |
| J1256569+014616 | 12 56 56.94 | +01 46 16.9 | 1996.372 | 18.20 | 3.77 | 1.49 | 0.17 | 0.09 | 0.13 |
| J1359551–403456 | 13 59 55.11 | –40 34 56.5 | 1996.393 | 16.98 | 3.20 | 1.16 | 0.10 | 0.10 | 0.13 |
| J1411051–791536 | 14 11 05.16 | –79 15 36.0 | 1996.366 | 16.23 | 3.10 | 1.06 | 0.07 | 0.08 | 0.10 |
| J1446229–395231 | 14 46 22.96 | –39 52 31.3 | 1998.540 | 17.67 | 3.37 | 1.23 | 0.17 | 0.14 | 0.16 |
| J1520174–175530 | 15 20 17.46 | –17 55 30.5 | 2000.566 | 17.80 | 3.40 | 0.92 | 0.16 | 0.15 | 0.21 |
| J1622326–120719 | 16 22 32.68 | –12 07 19.0 | 1997.263 | 16.56 | 3.20 | 0.89 | 0.07 | 0.08 | 0.13 |
| J1633131–755322 | 16 33 13.13 | –75 53 22.8 | 1999.633 | 16.20 | 3.10 | 1.10 | 0.06 | 0.07 | 0.10 |
| J1647383–115608 | 16 47 38.33 | –11 56 08.9 | 1999.584 | 18.08 | 4.23 | 2.05 | 0.17 | 0.10 | 0.09 |
| J1707252–013809 | 17 07 25.27 | –01 38 09.2 | 2000.566 | 17.81 | 3.55 | 1.40 | 0.15 | 0.12 | 0.14 |
| J1716352–031542 | 17 16 35.23 | –03 15 42.5 | 2001.378 | 14.46 | 3.43 | 1.71 | 0.05 | 0.10 | 0.09 |
| J1753452–655955 | 17 53 45.25 | –65 59 55.1 | 1996.667 | 17.80 | 3.59 | 1.79 | 0.14 | 0.10 | 0.12 |
| J1901391–370017 | 19 01 39.11 | –37 00 17.5 | 1999.433 | 17.94 | 3.71 | 1.94 | 0.16 | 0.11 | 0.10 |
| J1907440–282420 | 19 07 44.01 | –28 24 20.3 | 1999.748 | 17.95 | 3.60 | 0.97 | 0.16 | 0.12 | 0.18 |
| J1934511–184134 | 19 34 51.19 | –18 41 34.8 | 2000.568 | 17.71 | 3.43 | 1.15 | 0.14 | 0.11 | 0.16 |
| J2013108–124244 | 20 13 10.83 | –12 42 44.8 | 1998.584 | 18.07 | 3.55 | 1.21 | 0.17 | 0.15 | 0.17 |
| J2126340–314322 | 21 26 34.00 | –31 43 22.1 | 1998.652 | 16.26 | 3.06 | 0.91 | 0.07 | 0.13 | 0.16 |
| J2139136–352950 | 21 39 13.65 | –35 29 50.6 | 1996.691 | 17.94 | 3.47 | 1.11 | 0.17 | 0.11 | 0.20 |
| J2143510–833712 | 21 43 51.04 | –83 37 12.5 | 1998.529 | 16.50 | 3.30 | 0.98 | 0.10 | 0.06 | 0.11 |
| J2150133–661036 | 21 50 13.30 | –66 10 36.8 | 1998.608 | 17.23 | 3.55 | 1.13 | 0.14 | 0.08 | 0.12 |
| J2150149–752035 | 21 50 14.97 | –75 20 35.8 | 1998.518 | 17.45 | 3.51 | 1.39 | 0.16 | 0.09 | 0.12 |
| J2243169–593219 | 22 43 16.99 | –59 32 19.8 | 1998.841 | 17.40 | 3.32 | 1.11 | 0.15 | 0.10 | 0.14 |
| J2308113–272200 | 23 08 11.30 | –27 22 00.6 | 1998.789 | 18.11 | 3.53 | 1.40 | 0.20 | 0.17 | 0.17 |
| J2345390+005514 | 23 45 39.05 | +00 55 14.4 | 1998.718 | 16.90 | 3.18 | 1.28 | 0.12 | 0.13 | 0.13 |

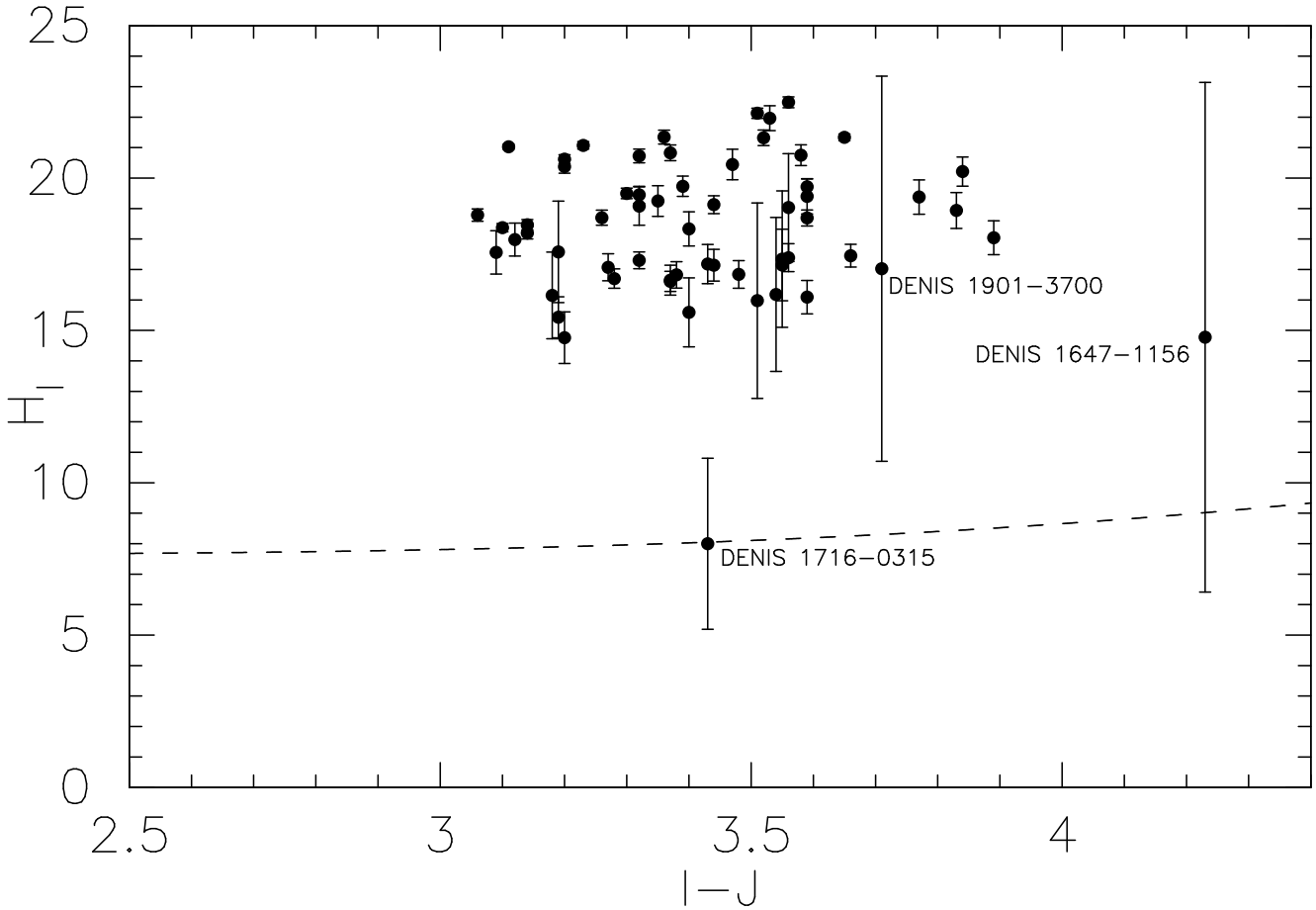


Fig. 3 I -band reduced proper motions versus $I - J$. The dashed curve represents the maximum possible reduced proper motion for a giant at a given color, H_I^{\max} . Objects well above this curve (e.g., $> 3\sigma$) must be dwarfs. Two objects classified as red, distant stars are indicated: DENIS 1647–1156 and DENIS 1716–0315. DENIS 1901–3700 is above the curve but within 2σ , see § 5 for further discussion.

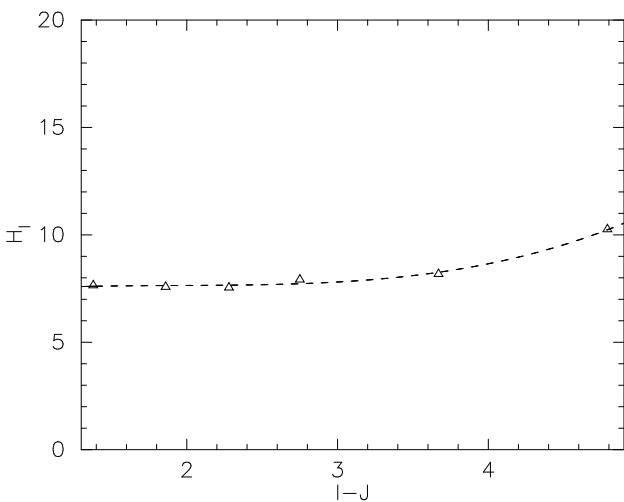


Fig. 2 $(H_I^{\max}, I - J)$ I -band maximum reduced proper motions-color diagram for red giants, plotted as open triangles, data from Bessell & Brett (1988); Fluks et al. (1994); Thé et al. (1990). The dashed curve represents our cubic least-square fit to the data.

cooler giants from Fluks et al. (1994) to the Bessell & Brett (1988); Thé et al. (1990) sample used in Phan-Bao et al. (2003). The following cubic least-square fit (see Fig. 2) is valid for $3.0 \leq I - J \leq 4.5$, or dwarf spectral types between M8.0 and L8.0:

$$H_I^{\max} = 6.79 + 1.25(I - J) - 0.630(I - J)^2 + 0.108(I - J)^3 \quad (2)$$

The rms dispersion around the fit is 0.1 mag.

Figure 3 shows the position of the resulting H_I^{\max} vs. $(I - J)$ curve relative to the 60 candidates. The curve classifies 57 candidates as nearby late-M and L dwarfs (Table 2). DENIS 1901–3700 (further discussed in § 5) is in the dwarf part of the diagram but within 2σ of the limit. The remaining two (see Table 3) are within 1σ , they are therefore likely red, distant objects. Nineteen of the 57 ultracool dwarfs have proper motions under $0.1''\text{yr}^{-1}$, giving a significant $\sim 33\%$ fraction of low-pm ultracool dwarfs in our sample.

Table 2. 57 nearby L, and late-M dwarfs and a member candidate of R-CrA (DENIS 1901–3700)

| DENIS name | Other name | Time | No. of | μ RA | err μ RA | μ DE | err μ DE | H_I | err H_I | H_I^{\max} | d | err d | SpT | V_t | Refs. |
|--------------|--------------|-----------|--------|----------------------|----------------------|----------------------|----------------------|-------|-----------|--------------|------|---------|------|--------------------|-------|
| (1) | (2) | b.l. (yr) | obs. | ("yr ⁻¹) | ("yr ⁻¹) | ("yr ⁻¹) | ("yr ⁻¹) | (mag) | (mag) | (mag) | (pc) | (pc) | (14) | km s ⁻¹ | (16) |
| D* 0000–1245 | 2M 0000–1245 | 5.066 | 5 | -0.143 | 0.050 | -0.126 | 0.027 | 17.6 | 0.7 | 7.8 | 23.1 | 4.4 | M9.0 | 20.9 | 5 |
| D* 0006–6436 | | 6.941 | 3 | 0.094 | 0.005 | -0.033 | 0.013 | 16.7 | 0.3 | 7.9 | 21.9 | 3.9 | L0.0 | 10.3 | |
| D* 0014–4844 | | 13.231 | 4 | 0.936 | 0.013 | 0.278 | 0.030 | 22.5 | 0.2 | 8.1 | 19.1 | 3.3 | L2.0 | 88.4 | |
| D* 0028–1927 | | 15.022 | 4 | 0.093 | 0.008 | 0.002 | 0.016 | 17.5 | 0.4 | 8.2 | 16.3 | 3.6 | L3.0 | 7.2 | |
| D* 0031–3840 | S* 0031–3840 | 17.912 | 5 | 0.542 | 0.027 | -0.098 | 0.015 | 21.3 | 0.3 | 8.1 | 21.4 | 3.9 | L2.0 | 55.9 | 1 |
| D* 0050–1538 | S* 0050–1538 | 16.044 | 5 | -0.243 | 0.022 | -0.443 | 0.019 | 20.4 | 0.2 | 7.9 | 26.9 | 5.0 | M9.0 | 64.4 | 1,5 |
| D* 0053–3631 | | 13.345 | 4 | 0.032 | 0.007 | -0.092 | 0.015 | 18.0 | 0.6 | 8.5 | 13.4 | 2.6 | L4.0 | 6.2 | |
| D* 0055–5450 | | 19.096 | 5 | -0.077 | 0.011 | 0.041 | 0.007 | 16.8 | 0.4 | 8.0 | 22.1 | 5.1 | L1.0 | 9.1 | |
| D* 0116–6455 | | 6.038 | 4 | -0.171 | 0.013 | -0.274 | 0.052 | 20.4 | 0.5 | 8.1 | 26.7 | 4.9 | L1.0 | 40.9 | |
| D* 0128–5545 | 2M 0128–5545 | 15.968 | 4 | -0.210 | 0.007 | 0.028 | 0.013 | 18.7 | 0.2 | 7.9 | 26.8 | 5.2 | L0.0 | 26.9 | 2 |
| D* 0147–4954 | 2M 0147–4954 | 21.951 | 5 | -0.065 | 0.008 | -0.261 | 0.014 | 18.2 | 0.2 | 7.8 | 20.4 | 3.7 | M9.0 | 26.0 | 3 |
| D* 0206–0735 | | 11.082 | 3 | -0.043 | 0.006 | 0.003 | 0.022 | 16.1 | 0.5 | 8.2 | 21.5 | 4.1 | L2.0 | 4.4 | |
| D* 0213–1343 | | 11.956 | 3 | -0.286 | 0.020 | -0.471 | 0.005 | 21.3 | 0.2 | 8.0 | 29.1 | 6.2 | L1.0 | 76.0 | |
| D* 0227–1624 | S* 0227–1624 | 8.836 | 4 | 0.472 | 0.023 | -0.324 | 0.035 | 20.8 | 0.3 | 8.0 | 21.7 | 4.2 | L1.0 | 58.9 | 1 |
| D* 0230–0953 | | 2.056 | 3 | 0.144 | 0.103 | -0.002 | 0.035 | 19.0 | 1.8 | 8.1 | 26.3 | 5.8 | L2.0 | 18.0 | |
| D* 0240–5305 | | 5.824 | 3 | 0.138 | 0.022 | 0.032 | 0.011 | 18.9 | 0.6 | 8.4 | 15.4 | 2.8 | L4.0 | 10.3 | |
| D* 0254–1934 | 2M 0254–1934 | 3.246 | 5 | 0.180 | 0.127 | -0.008 | 0.102 | 17.6 | 1.7 | 7.9 | 21.1 | 3.7 | M9.0 | 18.0 | 7 |
| D* 0301–5903 | | 15.899 | 4 | 0.088 | 0.014 | -0.031 | 0.011 | 16.6 | 0.5 | 8.0 | 19.4 | 3.4 | L1.0 | 8.6 | 4 |
| D* 0304–2435 | | 13.039 | 4 | 0.010 | 0.023 | -0.100 | 0.005 | 17.3 | 0.3 | 7.9 | 26.7 | 4.8 | L0.0 | 12.7 | |
| D* 0325–4312 | | 5.883 | 4 | 0.085 | 0.023 | -0.191 | 0.040 | 19.1 | 0.6 | 7.9 | 29.1 | 5.4 | L0.0 | 28.8 | |
| D* 0407–2348 | 2M 0407–2348 | 15.104 | 5 | -0.039 | 0.012 | -0.003 | 0.022 | 14.8 | 0.8 | 7.9 | 26.2 | 5.4 | M9.0 | 4.9 | 5 |
| D* 0419–4025 | | 18.900 | 5 | 0.040 | 0.018 | -0.020 | 0.011 | 15.6 | 1.1 | 8.0 | 23.6 | 4.3 | L1.0 | 5.0 | |
| D* 0427–1127 | | 45.995 | 5 | -0.007 | 0.007 | -0.229 | 0.004 | 18.5 | 0.2 | 7.8 | 27.1 | 4.7 | M9.0 | 29.4 | |
| D* 0436–4218 | 2M 0436–4218 | 5.987 | 4 | 0.033 | 0.031 | 0.028 | 0.036 | 16.2 | 2.5 | 8.1 | 24.5 | 4.7 | L2.0 | 5.0 | 7 |
| D* 0501–7705 | | 22.934 | 5 | 0.078 | 0.006 | 0.056 | 0.017 | 17.1 | 0.4 | 7.9 | 27.4 | 5.1 | L0.0 | 12.5 | |
| D* 0526–4455 | 2M 0526–4455 | 19.187 | 4 | 0.030 | 0.007 | -0.161 | 0.008 | 18.7 | 0.3 | 8.2 | 18.7 | 3.4 | L2.0 | 14.5 | 2 |
| D* 0605–2342 | 2M 0605–2342 | 6.142 | 5 | -0.014 | 0.048 | 0.039 | 0.045 | 16.0 | 3.2 | 8.1 | 24.7 | 4.4 | L2.0 | 4.9 | 5 |
| D* 0624–4521 | 2M 0624–4521 | 5.663 | 3 | -0.040 | 0.031 | 0.236 | 0.027 | 20.2 | 0.5 | 8.4 | 16.2 | 3.1 | L4.0 | 18.4 | 3 |
| D* 0627–3919 | | 6.677 | 3 | 0.064 | 0.011 | -0.132 | 0.027 | 18.3 | 0.6 | 8.0 | 25.4 | 4.8 | L1.0 | 17.7 | |
| D* 0641–4322 | S* 0641–4322 | 17.263 | 4 | 0.228 | 0.008 | 0.621 | 0.011 | 21.1 | 0.1 | 7.9 | 26.9 | 4.7 | L0.0 | 84.3 | 1 |
| D* 0703–6110 | | 6.964 | 3 | 0.070 | 0.009 | 0.005 | 0.024 | 17.1 | 0.5 | 8.0 | 28.4 | 5.4 | L1.0 | 9.4 | |
| D* 0719–5051 | | 12.041 | 3 | 0.205 | 0.017 | -0.073 | 0.007 | 19.1 | 0.3 | 8.0 | 22.9 | 4.1 | L1.0 | 23.6 | |
| D* 0921–2104 | S* 0921–2104 | 16.892 | 5 | 0.266 | 0.010 | -0.889 | 0.006 | 21.3 | 0.1 | 8.2 | 10.0 | 1.7 | L3.0 | 44.0 | 1,3 |
| D* 1019–2707 | S* 1019–2707 | 13.937 | 4 | -0.580 | 0.033 | -0.053 | 0.011 | 20.7 | 0.2 | 7.9 | 22.3 | 3.9 | L0.0 | 61.6 | 1,2 |
| D* 1115–2429 | | 8.017 | 4 | -0.001 | 0.024 | -0.198 | 0.042 | 18.0 | 0.5 | 7.8 | 25.8 | 4.4 | M9.0 | 24.2 | |
| D* 1206–3937 | | 4.844 | 3 | 0.193 | 0.025 | -0.074 | 0.026 | 19.2 | 0.5 | 8.0 | 30.1 | 5.5 | L0.0 | 29.5 | |
| D* 1234–1124 | | 12.977 | 4 | -0.137 | 0.023 | -0.104 | 0.020 | 19.4 | 0.6 | 8.2 | 24.6 | 4.9 | L2.0 | 20.1 | |
| D* 1256+0146 | | 13.959 | 3 | -0.160 | 0.029 | -0.063 | 0.011 | 19.4 | 0.6 | 8.3 | 17.4 | 3.1 | L4.0 | 14.2 | |
| D* 1359–4034 | | 5.961 | 3 | 0.066 | 0.011 | -0.531 | 0.010 | 20.6 | 0.1 | 7.9 | 28.4 | 5.2 | M9.0 | 72.0 | |

Table 2. Continued

| DENIS name | Other name | Time | No. of | μ RA | err μ RA | μ DE | err μ DE | H_I | err H_I | H_I^{\max} | d | err d | SpT | V_t | Refs. |
|---------------------------|--------------|-----------|--------|----------------------|----------------------|----------------------|----------------------|-------|-----------|--------------|------|---------|------|--------------------|-------|
| (1) | (2) | b.l. (yr) | obs. | ("yr ⁻¹) | ("yr ⁻¹) | ("yr ⁻¹) | ("yr ⁻¹) | (mag) | (mag) | (mag) | (pc) | (pc) | (14) | km s ⁻¹ | (16) |
| D* 1411–7915 | | 14.989 | 4 | −0.258 | 0.005 | −0.073 | 0.012 | 18.4 | 0.1 | 7.8 | 23.5 | 4.1 | M9.0 | 29.9 | |
| D* 1446–3952 | | 17.095 | 3 | 0.061 | 0.004 | −0.007 | 0.005 | 16.6 | 0.3 | 8.0 | 29.0 | 5.9 | L1.0 | 8.4 | |
| D* 1520–1755 | | 6.666 | 5 | −0.015 | 0.041 | −0.243 | 0.017 | 19.7 | 0.3 | 8.0 | 29.7 | 6.2 | L1.0 | 34.3 | |
| D* 1622–1207 | | 6.762 | 3 | 0.020 | 0.024 | −0.056 | 0.009 | 15.4 | 0.7 | 7.9 | 23.8 | 4.2 | M9.0 | 6.7 | |
| D* 1633–7553 | | 13.775 | 5 | −0.113 | 0.009 | −0.917 | 0.008 | 21.0 | 0.1 | 7.8 | 22.8 | 3.9 | M9.0 | 99.9 | |
| D* 1707–0138 | | 12.115 | 4 | 0.070 | 0.031 | −0.023 | 0.017 | 17.1 | 1.2 | 8.1 | 22.0 | 4.3 | L2.0 | 7.7 | |
| D* 1753–6559 | 2M 1753–6559 | 7.760 | 4 | −0.063 | 0.020 | −0.384 | 0.033 | 20.8 | 0.3 | 8.1 | 20.7 | 3.8 | L2.0 | 38.2 | 3 |
| D* 1901–3700 ^a | | 19.012 | 4 | 0.009 | 0.144 | −0.065 | 0.168 | 17.0 | 6.3 | 8.3 | | | | | 8 |
| D* 1907–2824 | | 11.064 | 3 | 0.091 | 0.014 | −0.206 | 0.006 | 19.7 | 0.3 | 8.2 | 21.8 | 4.2 | L2.0 | 23.3 | |
| D* 1934–1841 | | 8.869 | 3 | 0.076 | 0.016 | −0.019 | 0.011 | 17.2 | 0.6 | 8.0 | 26.4 | 5.0 | L1.0 | 9.8 | |
| D* 2013–1242 | | 3.937 | 3 | 0.025 | 0.077 | −0.067 | 0.044 | 17.3 | 2.2 | 8.1 | 24.8 | 5.1 | L2.0 | 8.4 | |
| D* 2126–3143 | | 13.789 | 4 | 0.214 | 0.017 | −0.238 | 0.011 | 18.8 | 0.2 | 7.8 | 25.2 | 5.0 | M8.0 | 38.2 | |
| D* 2139–3529 | | 16.019 | 3 | 0.012 | 0.010 | −0.059 | 0.006 | 16.8 | 0.5 | 8.1 | 26.7 | 5.0 | L1.0 | 7.6 | |
| D* 2143–8337 | | 6.073 | 5 | 0.336 | 0.002 | −0.212 | 0.022 | 19.5 | 0.2 | 7.9 | 19.2 | 3.2 | L0.0 | 36.2 | 6 |
| D* 2150–6610 | | 10.998 | 4 | −0.073 | 0.007 | 0.079 | 0.015 | 17.4 | 0.5 | 8.1 | 16.5 | 2.9 | L2.0 | 8.4 | |
| D* 2150–7520 | S* 2150–7520 | 6.820 | 3 | 0.839 | 0.001 | −0.198 | 0.009 | 22.1 | 0.2 | 8.1 | 20.1 | 3.6 | L2.0 | 82.1 | 1 |
| D* 2243–5932 | 2M 2243–5932 | 13.971 | 4 | −0.019 | 0.010 | −0.256 | 0.015 | 19.4 | 0.3 | 7.9 | 28.1 | 5.2 | L0.0 | 34.2 | 2 |
| D* 2308–2722 | S* 2308–2721 | 4.019 | 4 | 0.550 | 0.040 | −0.214 | 0.054 | 22.0 | 0.4 | 8.1 | 26.3 | 5.7 | L2.0 | 73.6 | 1 |
| D* 2345+0055 | | 9.880 | 4 | 0.050 | 0.040 | −0.050 | 0.020 | 16.1 | 1.4 | 7.9 | 28.3 | 5.6 | M9.0 | 9.5 | |

Abbreviations.—D*: DENIS; 2M: 2MASS; S*: SIPS.

Cols. (1) & (2): abbreviated DENIS name and other names.

Cols. (3) & (4): number of observations and time baseline.

Cols. (5)–(8): proper motions and associated errors.

Cols. (9) & (10): I -band reduced proper motion and associated error.

Col. (11): maximum reduced proper motion for an M giant of the same $I - J$ color.

Cols. (12) & (13): photometric distance and its standard error.

Col. (14): spectral type.

Col. (15): tangential velocities.

References. —(1): Deacon, Hambly & Cooke (2005); (2): Kendall et al. (2007); (3): Reid et al. (2006); (4): Bouy et al. (2003); (5): Cruz et al. (2007);

(6): Delfosse et al. (1999); (7): Reid et al. (2008); (8): Martín et al. (2010).

^a: A member candidate of the Corona Australis (R-CrA) molecular cloud complex (Martín et al. 2010), see § 5 for further discussion.

Table 3 2 red, distant objects

| DENIS name | Other name | Time b.l. (yr) | No. of obs. | μ RA ("yr ⁻¹) | err μ RA ("yr ⁻¹) | μ DE ("yr ⁻¹) | err μ DE ("yr ⁻¹) | H_I (mag) | err H_I (mag) | H_I^{\max} (mag) |
|--------------|------------|-------------------|----------------|----------------------------------|--------------------------------------|----------------------------------|--------------------------------------|----------------|--------------------|-----------------------|
| (1) | (2) | (3) | (4) | (5) | (6) | (7) | (8) | (9) | (10) | (11) |
| D* 1647–1156 | | 3.270 | 3 | 0.021 | 0.074 | –0.006 | 0.041 | 14.8 | 8.4 | 9.0 |
| D* 1716–0315 | | 46.800 | 5 | –0.005 | 0.006 | 0.001 | 0.003 | 8.0 | 2.8 | 8.0 |

5 DISCUSSION

Figure 3 demonstrates that the final target sample was only little ($\sim 3\%$) contaminated by distant red objects. The large majority of distant red objects had been previously rejected by the $(I - J, J - K)$ color-color filtering and the literature check. The faint I -band magnitudes of the remaining candidates ($I \geq 16$) which could not be associated with a known giant star made it unlikely that they could be unrecognized ones: a giant with $I - J \geq 3.0$ ($\sim M8$) has an I -band absolute magnitude $M_I \geq -3.0$ (Fluks et al. 1994), which for $I \geq 16$ gives a minimum distance of ~ 60 kpc, outside our Galaxy. Finally, our restriction to high Galactic latitudes ($|b_{\text{II}}| \geq 15^\circ$) and our rejection of objects which overlap known molecular complexes (mostly) eliminated reddened bright stars as contaminants. Within those restrictions, and for application where a small residual contamination is acceptable, one could thus in principle dispense with the MRPM filtering.

Using our M_J vs. $I - J$ calibration, we estimated distances for all 57 ultracool dwarfs, and then computed tangential velocities, (see Table 2). One should note that Table 2 does not list these estimates for DENIS 1901–3700, a member candidate of the R-CrA molecular cloud region (Martín et al. 2010) (see below). Four of the dwarfs have V_t above 80 km s^{-1} (DENIS 0014–4844, DENIS 0641–4322, DENIS 1633–7553, and DENIS 2150–7520), and could thus have reduced metallicities. All ultracool subdwarfs ($I - J \geq 2.0$, later than $\sim \text{sdM9}$) known to date however have $J - K < 0.7$ (e.g., Table 7 in Burgasser, Cruz & Kirkpatrick 2007 and references therein). The $J - K \geq 0.89$ of these four stars therefore make it unlikely that they are true subdwarfs, they could still have somewhat subsolar metallicities.

One should note that some of the 57 ultracool dwarfs could be unresolved binaries, whose distances are underestimated by up to $\sqrt{2}$. Reid et al. (2006) recently reported that DENIS 0147–4954 (as 2MASS 0147–4954) is an M8+L2 binary.

We estimate spectral types for the 57 ultracool dwarfs from their $I - J$ color. A linear least-squares fit (Fig. 4) to the data of 34 late-M, and L dwarfs (Table 1 in Phan-Bao et al. 2008) gives the following color-spectral type relation: $\text{SpT} = 7.39(I - J) - 14.28$, $\sigma = 0.87$, where SpT is the spectral subtype, counted from 8.0 for spectral type M8.0 to 18.0 for spectral type L8.0. Table 2 lists the resulting spectral types for the 57 ultracool dwarfs, with a standard error of about

1 subclass. Figure 5 shows a comparison of our estimated spectral types of 43 ultracool dwarfs with the spectroscopically determined ones of Martín et al. (2010). Some objects have large deviations, e.g., DENIS 0240–5305 and DENIS 1359–4034, clearly due to large photometric uncertainties.

DENIS 1901–3700 is above our MRPM curve within 2σ . The large relative error on its proper motion makes its true position in the $(H_I, I - J)$ diagram uncertain, reddening probably contributes to that situation as the object lies just outside our mask for the R Coronae Australis molecular cloud. The extremely red color of DENIS 1901–3700 ($I - J = 3.71$) likely reflects a combination of reddening with a red intrinsic spectrum. Martín et al. (2010) reported that DENIS 1901–3700 has a low surface gravity and M8 spectral type and is a member candidate of the R-CrA region. However its spectrum does not show strong H α emission as seen in DENIS-P J1859509–370632 (Bouy et al. 2004). Further observations are required to confirm its membership in R-CrA or its status as a background star.

DENIS 1647–1156 is above the MRPM curve within 1σ and it is a reddened main sequence star (M. Bessell, private communication). As the star is in the general vicinity of the LDN 204B dark nebula, it is probably reddened by dust associated with that region. DENIS 1716–0315 lies on the curve and the source is a giant star (Martín et al. 2010). This results in a fraction of about 3% contaminated by red, distant stars in our sample of nearby ultracool dwarfs.

6 SUMMARY

In this paper, we have shown how to use the MRPM method to detect 57 nearby L and late-M dwarfs in the DENIS database. We measured proper motions of these ultracool dwarfs: 38 with high-pm and 19 with low-pm, giving a significant $\sim 33\%$ fraction of low-pm ultracool dwarfs in our sample. These sources are in the solar neighborhood and cooler than M8. They are therefore new targets for a search of planets around ultracool dwarfs. Their detection demonstrates the success of the MRPM method that can be used in the future to complete the search of nearby ultracool dwarfs in the Galactic plane (the northern hemisphere part).

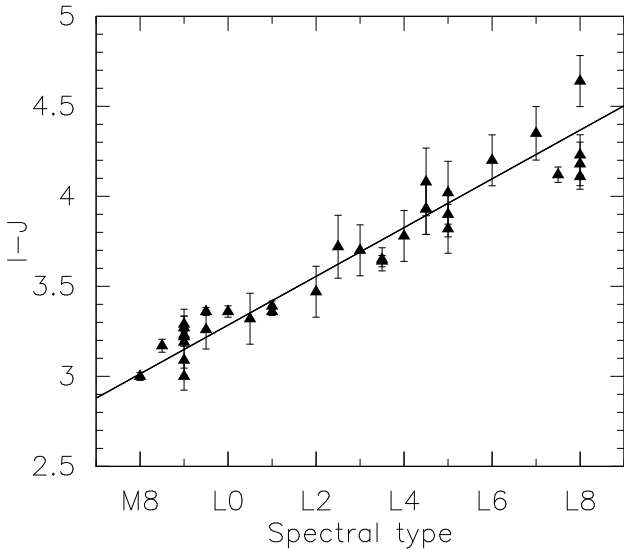


Fig. 4 Color-spectral type diagram for 34 late-M ($\geq M8.0$) and L dwarfs, plotted as solid triangles (data in Table 1 of Phan-Bao et al. 2008).

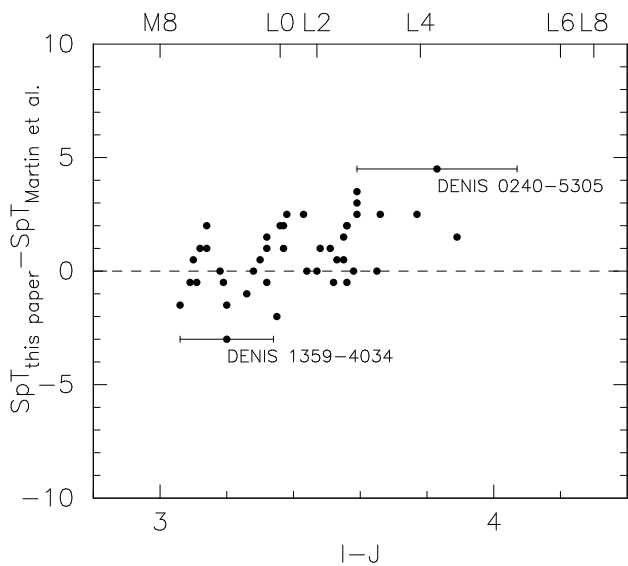


Fig. 5 Comparison of our photometrically estimated spectral types of 43 ultracool dwarfs with the spectroscopically determined ones of Martín et al. (2010). Two objects DENIS 0240–5305 and DENIS 1359–4034, which have large deviations, are indicated with error bars on the $I - J$ color.

Acknowledgments

The DENIS project has been partly funded by the SCIENCE and the HCM plans of the European Commission under grants CT920791 and CT940627. It is supported by INSU, MEN and CNRS in France, by the State of Baden-Württemberg in Germany, by DGICYT in Spain, by CNR in Italy, by FFwFBWF in Austria, by FAPESP in Brazil, by OTKA grants F-4239 and F-013990 in Hungary, and by the ESO C&EE grant A-04-046. Jean Claude Renault from IAP was the project

manager. Observations were carried out thanks to the contribution of numerous students and young scientists from all involved institutes, under the supervision of P. Fouqué, survey astronomer resident in Chile.

The Digitized Sky Surveys were produced at the Space Telescope Science Institute under U.S. Government grant NAG W-2166. The images of these surveys are based on photographic data obtained using the Oschin Schmidt Telescope on Palomar Mountain and the UK Schmidt Telescope. The plates were processed into the present compressed digital form with the permission of these institutions. The National Geographic Society - Palomar Observatory Sky Atlas (POSS-I) was made by the California Institute of Technology with grants from the National Geographic Society. The Second Palomar Observatory Sky Survey (POSS-II) was made by the California Institute of Technology with funds from the National Science Foundation, the National Geographic Society, the Sloan Foundation, the Samuel Oschin Foundation, and the Eastman Kodak Corporation. The Oschin Schmidt Telescope is operated by the California Institute of Technology and Palomar Observatory. The UK Schmidt Telescope was operated by the Royal Observatory Edinburgh, with funding from the UK Science and Engineering Research Council (later the UK Particle Physics and Astronomy Research Council), until 1988 June, and thereafter by the Anglo-Australian Observatory. The blue plates of the southern Sky Atlas and its Equatorial Extension (together known as the SERC-J), as well as the Equatorial Red (ER), and the Second Epoch [red] Survey (SES) were all taken with the UK Schmidt. This publication makes use of data products from the Two Micron All Sky Survey, which is a joint project of the University of Massachusetts and Infrared Processing and Analysis Center/California Institute of Technology, funded by the National Aeronautics and Space Administration and the National Science Foundation; the NASA/IPAC Infrared Science Archive, which is operated by the Jet Propulsion Laboratory/California Institute of Technology, under contract with the National Aeronautics and Space Administration. This research has made use of the ALADIN, SIMBAD and VIZIER databases, operated at CDS, Strasbourg, France.

N.P.-B has been supported by Vietnam National University HCMC grant B2011-28-10.

References

- Bessell M. S., Brett J. M., 1988, *PASP*, 100, 1134
- Bertin E., Arnouts, S., 1996, *A&AS*, 117, 393
- Bouy H. et al., 2003, *AJ*, 126, 1526
- Bouy H. et al., 2004, *A&A*, 424, 213
- Burgasser A. J., Cruz K. L., Kirkpatrick J. D., 2007, *ApJ*, 657, 494
- Cioni M.-R. et al., 2000, *A&AS*, 144, 235
- Cruz K. L. et al., 2003, *AJ*, 126, 2421
- Cruz K. L. et al., 2007, *AJ*, 133, 439

- Deacon N. R., Hambly N. C., Cooke J. A., 2005, *A&A*, 435, 363
- Delfosse X. et al., 1999, *A&AS*, 135, 41
- Epchtein N., 1997, in *The Impact of Large Scale Near-IR Sky Surveys*, (Dordrecht: Kluwer), ed. F. Garzon et al., 15
- Fluks M. A. et al., 1994, *A&AS*, 105, 311
- Kendall T. R. et al., 2007, *MNRAS*, 374, 445
- Kirkpatrick J. D. et al., 1999, *ApJ*, 519, 802
- Knapp G. R. et al., 2004, *AJ*, 127, 3553
- Lawrence A. et al., 2007, *MNRAS*, 379, 1599
- Leggett S. K., 1992, *ApJS*, 82, 531
- Lépine S., Shara M. M., Rich R. M., 2002, *AJ*, 124, 1190
- Lodieu N. et al., 2007, *MNRAS*, 379, 1423
- Martín E. L. et al., 1999, *AJ*, 118, 2466
- Martín E. L. et al., 2010, *A&A*, 517, A53
- Phan-Bao N. et al., 2001, *A&A*, 380, 590
- Phan-Bao N. et al., 2003, *A&A*, 401, 959
- Phan-Bao N. et al., 2008, *MNRAS*, 383, 831
- Pojmanski G., Maciejewski G., Pilecki B., Szczygiel D., 2005, *ASAS Variable Stars in Southern hemisphere* (Strasbourg: Vizier On-line Catalog)
- Reid I. N., Cruz K. L., 2002, *AJ*, 123, 2806
- Reid I. N. et al., 2006, *AJ*, 132, 891
- Reid I. N. et al., 2008, *AJ*, 136, 1290
- Samus N. N. et al., 2004, *Combined General Catalog of Variable Stars* (Strasbourg: Vizier On-line Catalog)
- Scholz R. D., Meusinger H., Jahreiß H., 2001, *A&A*, 374, L12
- Skrutskie M. F. et al., 1997, in *The Impact of Large Scale Near-IR Sky Surveys*, Kluwer Academic, Dordrecht, ed. Garzon F. et al., 25
- Thé P. S., Thomas D., Christensen C. G., Westerlund B. E., 1990, *PASP*, 102, 565
- York, D. G. et al., 2000, *AJ*, 120, 1579